Journal of Thermal Analysis and Calorimetry, Vol. 62 (2000) 633–645

STUDY OF Fe ADDITION ON THE THERMAL DECOMPOSITION OF COPRECIPITATED OXALATES FOR THE Bi-BASED SUPERCONDUCTOR SYNTHESIS

M. Popa[1], *J. M. Calderon-Moreno*[1], *D. Crisan*[2] *and M. Zaharescu*[2]

[1]Materials and Structures Laboratory, Tokyo Institute of Technology, Nagatsuta 4259, Midori-ku Yokohama 226-8503, Japan
[2]Romanian Academy, Institute of Physical Chemistry, Bucharest 77208, 202 Splaiul Independentei Romania

(Received December 22, 1999; in revised form July 27, 2000)

Abstract

This work introduces results obtained during the preparation of a Bi-based material with superconducting properties by oxalate coprecipitation.

The influence of Fe presence on the precursors thermal stability and on the superconducting phases formation mechanism are presented. The thermal decomposition and the stability in air of $FeC_2O_4 \cdot 2H_2O$ and also of the components mixture were studied by DTA/TG. It was evidenced that iron oxalate decomposes at the lowest temperature compared to the decomposition temperatures of the individual oxalates.

XRD, IR and TEM/ED studies were approached to investigate the individual oxalates and the mixture coprecipitates for the high-T_c superconducting material synthesis.

Keywords: Bi oxalate, Ca oxalate, coprecipitated BiSrCaCu oxalate, Cu oxalate, Fe oxalate, Sr oxalate, thermal decomposition

Introduction

The desire to achieve uniform, fine ceramic powders has generated a wide variety of methods for the powders preparation, among them wet chemical methods being the mostly used. The chemical methods increase the homogeneity of the product during the synthesis stages [1] and ensure a good stoichiometry and reproducibility. The high reactivity of the precursors permits also lower reaction temperatures and shorter reaction times. In order to have good superconducting properties, a widely accepted technique is to coprecipitate the metal ions as oxalates from the mixed salts solutions. The coprecipitation method is one of the known wet chemical routes most commonly used in the synthesis of high temperature superconducting oxides [2], leading to an intimate mixing of the components that cannot be obtained by grinding. It can also be mentioned that the oxalate coprecipitation is particularly important in Bi-based su-

1418–2874/2000/ $ 5.00

Akadémiai Kiadó, Budapest
Kluwer Academic Publishers, Dordrecht

perconductors preparation chemistry, especially for the production of high reactivity and homogeneous powders. This procedure yields compounds with the desired stoichiometry, a good crystallinity and of high purity. Coprecipitation is easy to perform, but requires a careful approach in order to produce a chemically homogeneous precipitate with the desired composition [3]. The success of the synthesis strongly depends on the control of the solution chemistry at every stage of the process. Based on literature data there are two ways of approaching the oxalate coprecipitation for the Bi-based superconducting materials synthesis: coprecipitation in a basic range of pH [4–8] and in an acid range of pH [9–13]. The coprecipitation in acid range leads to a precipitation of all metal ion species as oxalates, but reaching an optimum value of pH in order to achieve a quantitative precipitation still is a controversial problem of the method. The coprecipitation in basic range is less sensitive to the pH value, but leads to a mixture of coprecipitates that behaves differently in the subsequent thermal decomposition processes. The absorption of a quantity of alkali ions in the final precipitate is also possible or even to form some insoluble double salts.

The decomposition of coprecipitated salts is a good synthetic method for producing ceramic oxides and especially the Bi-based system was synthesized by this method [14].

The precipitation of Bi, Sr, Ca, Cu, Fe cations with $C_2O_4^{2-}$ anion are widely studied in the literature, but these complexes together in order to obtain a superconducting material have not been investigated in any detail. Although the thermal decomposition of the Bi, Sr, Ca, Cu and Fe oxalates has been the subject of a number of investigations [11, 13–22], the results and the conclusions that can be drawn are rather contradictory. The thermal effects as well as the types of the final products are substantially influenced by the working conditions, the atmosphere, the heating rates, the quantities of materials.

Following our research concerning the reactivity of Bi, Sr, Ca, Cu oxalate powders used in BSCCO preparation [13], this paper deals with the study of the thermal decomposition of coprecipitated salts, corresponding to the cations mentioned above, in the presence of Fe, under the conditions used to generate stable, homogeneous, ultrafine powders formed by 2223 as major phase. This work is a continuation of our research concerning the Cu substitutions by Fe [23] carried out in order to clarify more aspects about the formation mechanism of superconducting phases in the mentioned system, using Mössbauer spectroscopy; a special study was realized for the thermal decomposition of $FeC_2O_4{\cdot}2H_2O$ added to the mixture of the other cations salts. The literature contains few reports on the synthesis and thermal decomposition of iron oxalate [14, 16–21, 23] and to our knowledge there are no detailed studies of the Fe oxalate decomposition in the presence of Bi, Sr, Ca, Cu oxalates.

In our work, a special attention has been given to study the decomposition and oxidation of $FeC_2O_4{\cdot}2H_2O$ and to compare our results with those published in literature.

Experimental

Powders preparation

The samples were prepared by using stoichiometric amounts of starting materials corresponding to the formula $Bi_2Sr_2Ca_2Cu_3O_y$ and $Bi_2Sr_2Ca_2Cu_{3(1-x)}Fe_{3x}O_y$ (x=0.01), respectively. The way of approaching the preparation method in order to realize a complete coprecipitation of all components in the reaction mixture, as well as the applied thermal treatments to synthesize the superconducting material were discussed in previous papers [13, 23, 24]; mainly, 1 M nitric salts were used and the precipitation was realized at pH=3.5, by pouring the nitric salts in oxalic acid solution. The precipitation of $FeC_2O_4 \cdot 2H_2O$ was realized in the same manner.

The characterization of the oxalates and the thermally treated samples

The starting materials, as well as the thermally treated samples were characterized by XRD, TEM/ED, DTA/TG and IR. The structure of the obtained materials was determined by X-ray and electron diffraction. The X-ray diffraction patterns were recorded with a TUR M62 equipment with a HZ 63 θ-2θ diffractometer using CuK_α radiation monochromatized by a flat graphite crystal placed before the scintillation detector. Flow chart records were used to determine the phase compositions of the samples. Transmission electron microscopy and electron diffraction investigations were carried out using a JEOL transmission electron microscope operating at 200 kV. Samples for TEM were prepared in the following way: particles from powder material or crushed pellets were dispersed in a solution of formvar in alcohol on a glass plate. To establish the thermal events, DTA/TG was performed up to 1000°C in air, with Al_2O_3 as reference. A MOM OD-102 Derivatograph with a heating rate of 5°C min^{-1} was used. IR spectra were recorded in 4000–400 cm^{-1} range for the starting coprecipitates and in the range 2000–400 cm^{-1} for the thermally treated samples. A Carl Zeiss Jena-Specord 75 IR equipment was used.

Results and discussion

In previous studies we reported that the reaction between a solution of the corresponding metal nitrates and an alkaline solution of NaOH under certain conditions, yields stable, homogeneous, ultrafine coprecipitate of oxalates. A quantitative coprecipitation of individual oxalates and BiSrCaCuO mixture, respectively BiSrCaCuFeO, were studied in acid range of pH, at the value of 3.5. To obtain a good stoichiometry of the material, in our case, the pH value determined the complete and quantitative coprecipitation of all components and was established by previous experimental and theoretical works [13, 15, 25].

Studies on the initial powder of iron oxalate

XRD results of the initial powder of iron oxalate

After coprecipitation, yellow-coloured, ultrafine, very homogeneous, microcrystalline, well-dispersed particles of iron oxalate were synthesized. The results of XRD pattern of the powder (Fig. 1) are in good agreement with those from literature data, confirming the presence of $FeC_2O_4 \cdot 2H_2O$.

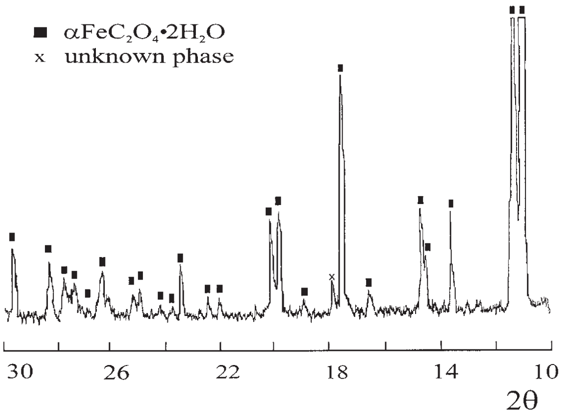

Fig. 1 The XRD pattern of the powder of $FeC_2O_4 \cdot 2H_2O$

TEM/ED results of the initial powder of $FeC_2O_4 \cdot 2H_2O$

A TEM/ED study was realized on the $FeC_2O_4 \cdot 2H_2O$ raw powder, as can be noticed in Fig. 2. Small-sized particles of $FeC_2O_4 \cdot 2H_2O$, with a high porosity have been obtained. A submicronic range of the crystallites was registered, with dimensions of 0.02 μm. Traces of Fe_2O_3 were present in the sample, due to the instability of the oxa-

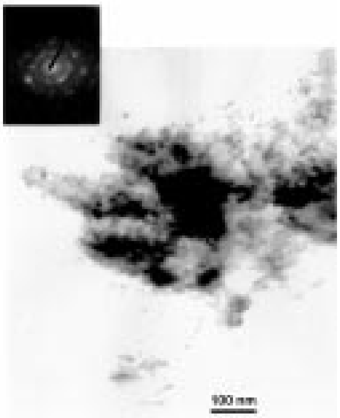

Fig. 2 The TEM micrograph together with the ED pattern of the $FeC_2O_4 \cdot 2H_2O$ powder

late in the electron beam during the TEM measurement. These results are in good accordance with the DTA/TG and XRD determinations.

DTA/TG results of the initial powder of $FeC_2O_4 \cdot 2H_2O$

In order to establish the thermal behaviour of the BSCCO oxalates mixture in the Fe presence, for the beginning, the thermal decomposition of $FeC_2O_4 \cdot 2H_2O$ was approached.

Table 1 Thermal effects attribution, mass loss and possible reactions of $FeC_2O_4 \cdot 2H_2O$

T_{range}/°C	Thermal effects		Mass loss/%		Effects attribution; possible reactions
	endo	exo	exp.	theoretic	
20–230	200	–	28.81	20	$FeC_2O_4 \cdot 2H_2O \rightarrow Fe_2O_4 + 2H_2O$
230–1000	–	310 420	32.20	44.44	$2FeC_2O_4 \rightarrow Fe_2O_3 + 2CO + 2CO_2$ $CO + 1/2O_2 \rightarrow CO_2$

The DTA and TG curves obtained for $FeC_2O_4 \cdot 2H_2O$ decomposition are presented in Fig. 3 and the obtained results are summarized in Table 1. The carried out investigations showed one endothermic effect and 2 exothermic effects on the DTA/TG curves, in contrast to [26], where only one exothermic effect was registered and in good agreement with [21]. The endothermic effect is related to the mass loss

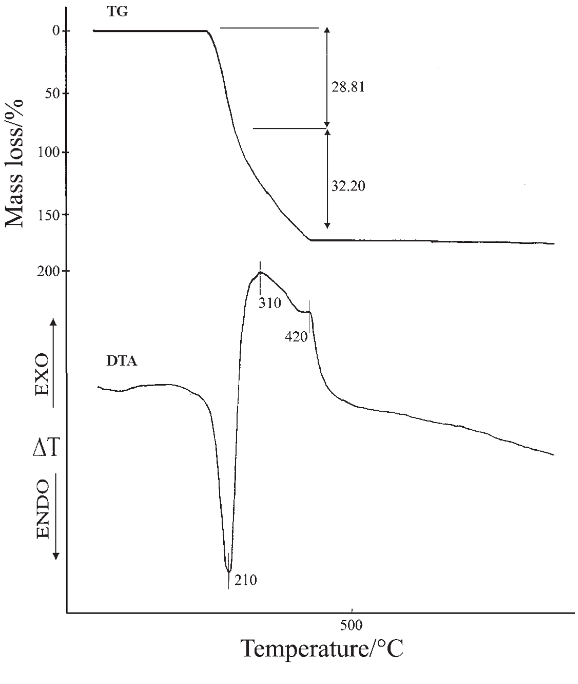

Fig. 3 The DTA/TG curves for $FeC_2O_4 \cdot 2H_2O$ at heating rate 10°C min^{-1}

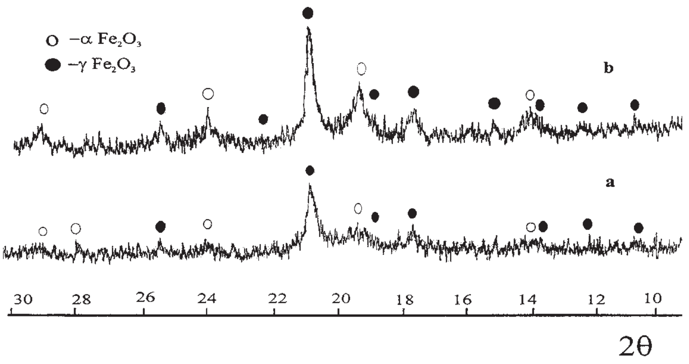

Fig. 4 The XRD pattern of the $FeC_2O_4 \cdot 2H_2O$ powder thermally treated at 300°C; a – without holding the temperature; b – holding temperature for 1 h

due to the $FeC_2O_4 \cdot 2H_2O$ dehydration. Up to 310°C, decomposition of the obtained FeC_2O_4 takes place with the formation of γ-Fe_2O_3, α-Fe_2O_3 and traces of Fe_3O_4 provided by X-ray phase analysis.

In Fig. 4a, b the X-ray patterns of the $FeC_2O_4 \cdot 2H_2O$ thermally treated at 300°C (Fig. 4a) are shown, confirming the presence of α-Fe_2O_3 obtained for the material maintained 1 h at the mentioned temperature (Fig. 4b). The process of decomposition of the oxalate takes place in the same time with the oxidation of Fe_3O_4 to Fe_2O_3 and CO to CO_2, as the effects on DTA curve showed. In contrast with [21] results, no increasing of mass was noticed. The thermal decomposition is accompanied by the exothermic effect due to the overlapping of the endothermic effect of the decomposition with the exothermic effect of the CO oxidation to CO_2.

Thermal decomposition results of the individual oxalates of Bi, Sr, Ca, Cu

Studies of XRD and DTA/TG were made on the initial powders of the individual oxalates. The XRD patterns for the individual oxalates are in good accordance with literature data [25], the presence of $Bi_2(C_2O_4)_3$, $SrC_2O_4 \cdot 2.5H_2O$, $CaC_2O_4 \cdot H_2O$, $CuC_2O_4 \cdot nH_2O$ being identified. The results concerning the $FeC_2O_4 \cdot 2H_2O$ decomposition were compared with those obtained previously for the Ca, Sr, Bi, Cu oxalates and are summarized in Table 2.

From the quantitative evaluation and the effects attribution results, the following conclusions could be drawn: the thermal decomposition of Bi oxalate takes place at 300°C, accompanied by an exothermic effect, with the Bi_2O_3 formation. The endothermic effect at 720°C corresponds to the phase transformation $\alpha \rightarrow \delta$ Bi_2O_3 and the effect at 800°C is due to melting of Bi_2O_3. The thermal decomposition of Sr and Ca oxalates is very similar. The Sr oxalate decomposition takes place at 490°C accompanied by an exothermic effect, with the formation of $SrCO_3$ which suffers a polymorphic transformation showed by the endothermic effect at 922°C. In the percentage mass loss can be noticed a significant difference between the experimentally calculated mass loss and the theoretical one. In dynamic conditions, as in the DTA experiment, $SrCO_3$ does not decompose totally even at 1000°C and even in the presence of Bi_2O_3, which in reaction with $SrCO_3$ determines an increase of the decomposition and decomposition rate of the carbonate. This is a reason why prolonged isothermal treatments are necessary. The Sr carbonate decomposition is promoted by the solid-state reaction with corresponding oxides; the SrO formation takes place between ~600–1000°C but it is not complete. Our result is in good concordance with previous works on Sr oxalate thermal decomposition [27, 28] and on the decarbonation of $SrCO_3$ in the presence of other oxides, where the incomplete decomposition of Sr carbonate at 1000°C was confirmed.

Table 2 Thermal effects attribution, mass loss and possible reactions of the oxalates of Bi, Sr, Ca, Cu

Temperature range/°C	Thermal effects		Mass loss/%		Effects attribution; possible reactions
	endo	exo	exp.	theor.	
			$Bi_2(C_2O_4)_3$		
20–200	–	–	2.07	–	humidity elimination
200–450	–	320	28.50	27.36	$Bi_2(C_2O_4)_3 \rightarrow Bi_2O_3+CO+CO_2$
450–1000	720	–	–	–	$\alpha\text{-}Bi_2O_3 \rightarrow \delta\text{-}Bi_2O_3$
	800	–	–	–	melting
20–1000	–	–	30.37	27.36	$Bi_2(C_2O_4)_3 \rightarrow Bi_2O_3$
			$SrC_2O_4 \cdot 2.5H_2O$		
20–300	110	–	–	–	
	200	–	21.21	20.40	$SrC_2O_4 \cdot 2.5H_2O \rightarrow SrC_2O_4+H_2O$
300–600	–	490	16.02	15.95	$SrC_2O_4 \rightarrow SrCO_3+CO$ $CO+1/2O_2 \rightarrow CO_2$
600–1000	900	–	20.30	29.80	$SrCO_3 \rightarrow SrO+CO_2$
	920	–	–	–	$SrCO_3$ rhombic→$SrCO_3$ hexagonal
20–1000	–	–	47.35	53.04	$SrC_2O_4 \rightarrow SrO$
			$CaC_2O_4 \cdot H_2O$		
20–300	190	–	13.79	12.32	$CaC_2O_4 \cdot H_2O \rightarrow CaC_2O_4+H_2O$
	270	–	–	–	
300–550	–	460	22.41	21.86	$CaC_2O_4 \rightarrow CaCO_3+CO$ $CO+1/2O_2 \rightarrow CO_2$
550–1000	760	–	43.43	43.96	$CaCO_3 \rightarrow CaO+CO_2$
20–1000	–	–	65.0	61.62	$CaC_2O_4 \cdot H_2O \rightarrow CaO$
			$CuC_2O_4 \cdot xH_2O$		
20–210	–	–	4.50	–	$CuC_2O_4 \cdot xH_2O \rightarrow CuC_2O_4+xH_2O$
210–300	–	300	58.48	58.07	$CuC_2O_4 \rightarrow Cu+2CO_2$
300–450	–	–	+22.72	+28.32	$Cu+O_2 \rightarrow CuO$
20–1000	–	–	56.77	–	$CuC_2O_4 \cdot xH_2O \rightarrow CuO$

Ca oxalate eliminates the humidity and the crystallization water in the temperature range of 20–300°C; this is associated with the endothermic effects at 190 and 270°C. The DTA curve of the decomposition of Ca oxalate presents an exothermic effect at 460°C, which reflects the decomposition of Ca oxalate together with $CaCO_3$ formation. The second mass loss between 300–550°C is assigned to the decomposition of CaC_2O_4 to $CaCO_3$ and CO. As the decomposition takes place in air, we assume that in both cases, for Sr and Ca oxalates, CO is oxidized simultaneous to CO_2. Because the exothermic effect of CO oxidation is higher than the endothermic effect of SrC_2O_4 and CaC_2O_4 thermal decomposition, the overall effect at 490 and 460°C respectively, is exothermic. Some disagreements are present in the literature concerning the CO oxidation to CO_2 in the thermal decomposition of simple and complex oxalates [29–31]. In our study, the chromatographic analysis of the gaseous products evidenced the presence of CO and CO_2 mixture. The gaseous products remain partially adsorbed on the solid phase and the desorption occurs stepwise, with increasing temperature [32, 33]. The endothermic effect at 730°C is accompanied by an important mass loss: 1 mol of CO_2 corresponds to the $CaCO_3$ decomposition and CaO formation. In the case of $CaC_2O_4{\cdot}H_2O$ decomposition the mass losses are in good concordance with the theoretical values and the literature data. The greater value of the total mass loss can be correlated to the higher humidity of the specimen. The decomposition of Cu oxalate starts immediately as the temperature begins to increase, the air-cooled coprecipitate containing moisture. After the water loss of the material, the decomposition of the anhydrous oxalate takes place in a single step with the maximum rate of decomposition at 300°C, in good agreement with the results obtained by [22]. The decomposition of the $CuC_2O_4{\cdot}xH_2O$ occurs in a single step and we assume that the exothermic effect on DTA curve indicates the decomposition of Cu oxalate to metallic Cu which simultaneously oxidizes to CuO [18, 34, 35]. The Cu oxalate yields Cu metal on thermal decomposition, which is confirmed by IR and TEM/ED results. In oxalates of the divalent metals, the M–O covalent bonds depend on the metal electronegativity. Decomposition occurs at a temperature where rupture of the M–O link is possible or at which rupture of the C–O bond nearest of the metal occurs. In the complex of Cu(II) as the Cu–O bond becomes stronger, the adjacent C–O bond becomes longer and exhibits a lower stretching frequency. This refers to the stability in solution and not the thermal stability in solid state [36]. The effects attributed to the Cu oxalate decomposition confirm the results that indicate the Cu obtaining and its oxidation at CuO. The difference between the values of the increasing in mass, experimentally calculated and the theoretically calculated corresponding to the oxidation of Cu at CuO can be explained taking into account the incomplete oxidation in the non-isothermal conditions applied.

We can conclude that the major decomposition step is related to the water loss between 190–270°C and the oxalates precipitates transformation to $CaCO_3$, $SrCO_3$, Bi_2O_3 and CuO between 320–490°C. The oxalates thermal decomposition is accompanied by an exothermic effect due to the superposition of the endothermic effect of the decomposition with the exothermic effect of the oxidation of CO to CO_2 [29–31]. Fe oxalate decomposes at the lowest temperature compared to the other studied oxalates.

Thermal decomposition and XRD results for the oxalates mixtures coprecipitates

In order to establish the formation mechanism of superconducting phases in the mentioned systems, the structure and thermal behaviour of the BSCCO and BSCCO–iron containing oxalates mixtures have also been studied. The XRD pattern for the four, respectively for the five components mixture certifies the presence of the mixture of Bi oxalate, Sr oxalate, Cu oxalate, respectively Fe oxalate and a mixture of (Sr, Ca) oxalate and certain amounts of amorphous phase.

The DTA/TG results corresponding to the mixtures of oxalates with and without Fe are presented in Fig. 5a, b. The similar behaviour of the materials can be observed. In both cases the thermal decomposition of the oxalates is finished below 500°C. As a result of this observation, according to DTA/TG results of the precursor materials, all oxalates were decomposed by thermal treatment at 600°C for 1 h, with the formation of oxides and carbonates CuO, Bi_2O_3, Fe_2O_3, $CaCO_3$ and $SrCO_3$; amounts of $CuBi_2O_4$ and $SrBi_4O_7$ were also identified [25]. The thermal decomposition of FeC_2O_4 takes place up to 400°C and the presence of Fe_2O_3 was detected. The thermal effects registered above 500°C are slowly shifted to higher temperatures, because of the Fe_2O_3 presence.

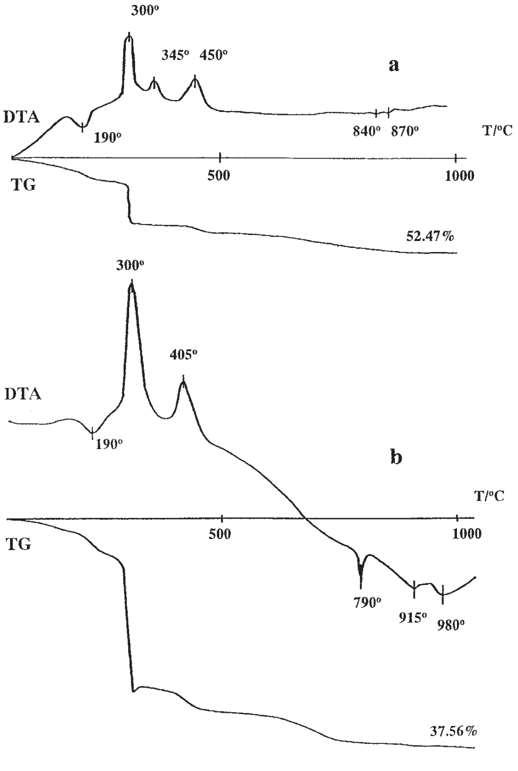

Fig. 5 The DTA/TG curves for; a – BSCCO; b – BSCCO+Fe

The IR results for the oxalates mixture coprecipitates

The IR results of the individual oxalates and four components mixture showed the characteristic bands of oxalate group. These bands are not evidenced in the spectrum of the thermal decomposition products. The characteristic bands of the carbonate group in the case of individual oxalates are evidenced at 1460–1400 ($\nu_{as}CO_3^{2-}$) cm^{-1}, ($\nu_sCO_3^{2-}$) cm^{-1}, 870–855 (δCO_3^{2-}) cm^{-1}. In the case of the samples resulted from the Bi and Cu individual oxalates, the characteristic bands of M–O bond at 545, 500, 430 (νBi–O) and 500 cm^{-1} (νCu–O) are present. The Ca and Sr oxalates generate the corresponding carbonates and Cu and Bi oxalates generate the corresponding oxides, which is in agreement with XRD previous results.

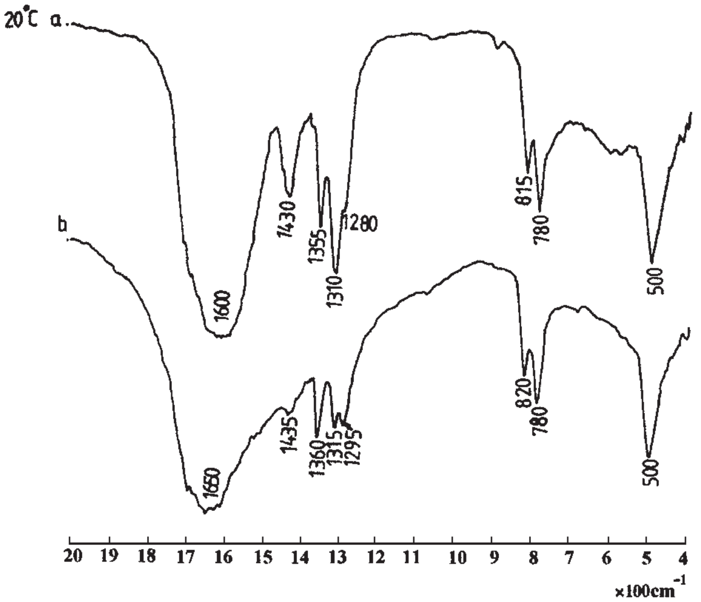

Fig. 6 The IR results for the initial coprecipitates; a – BSCCO, b – BSCCO+Fe

In Fig. 6 the IR spectra for the coprecipitated oxalates containing Bi, Sr, Ca, Cu and respectively Bi, Sr, Ca, Cu, Fe are shown. The multicomponent mixtures presented all the characteristic bands observed for the individual specimens. In the domain where M–O bond is present, some supplementary 'shoulders' appeared, a fact that can be correlated to the $CuBi_2O_4$ and $SrBi_4O_7$ phases formation, also observed in the XRD patterns [25].

The characteristic band assigned to ν_{as}(C=O) vibration at 1600 cm^{-1} in the coprecipitate without Fe is shifted at 1650 cm^{-1} in the Fe containing material. In the last case, the Fe–O bond is strong, while C–O bond is weaker; as a result, the double bond C=O is stronger and appears at energies significantly greater.

The weaker intensity of the band at 1435 cm^{-1} for the Fe doped material is associated to the decreasing of the energy bond C–O after the Fe–O bond is stabilized.

TEM/ED results for the BSCCO and BSCCO+Fe coprecipitates

The largest difficulty with the samples prepared by coprecipitation method was the instability occurred for the initial oxalates, which decomposed to the respective oxides when the beam was condensed onto the sample. The TEM micrographs for the raw material coprecipitates with and without Fe are presented in Fig. 7. The BSCCO sample presented uniform and homogeneous granulometric distribution of particles. A mixture of small, uniform, rod-like shape particles was noticed. The particles had dimensions in the range of 0.02–0.1 μm with an average value of 0.024 μm; a high porosity of the coprecipitate was also observed. The crystals have different shape and size.

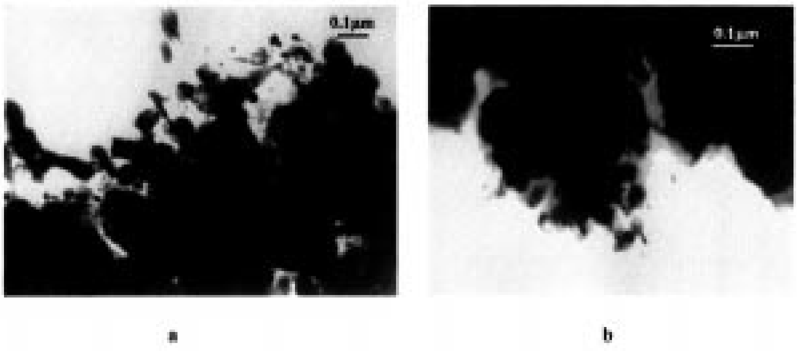

Fig. 7 The TEM curves of the initial coprecipitates; a – BSCCO; b – BSCCO+Fe

The Fe containing coprecipitate was crystallized, with an evident dispersion tendency of the crystalline phase. The coexistence of at least two phases was evidenced:

- platelet-like particles, with a regular shape, thick, with dimensions between 0.5–1.2 μm (for about 10% of the volume).
- small crystallites, rod-like shaped, with dimensions in the range of (0.02×0.1) μm<(diameter×length) μm<(0.1×0.3) μm.

Traces of Fe_2O_3 were noticed during TEM measurements. Compared to the BSCCO material, a more regular geometry of the particles was noticed in the case of Fe doped material. Also, an agglomeration tendency of the particles as well as an orientation of the acicular crystals were evidenced, effect induced by the Fe presence in the composition and by the decomposition of the material in the electron beam.

Conclusions

New aspects concerning the precipitation of Bi, Sr, Ca, Cu, Fe individual oxalates were discussed; we established the possibility of their quantitative precipitation at the same value of pH of 3.5.

The coprecipitation of the five components mixture leads to the obtaining of a mixture of oxalates with a lower solubility than in the case of the individual oxalates.

By coprecipitation, homogeneous submicronic, ultrafine powders have been obtained. The oxalates powders were high reactive and permitted the decrease of the thermal treatment temperatures and a high homogeneity of the final material.

The process of dehydration and decomposition of $FeC_2O_4{\cdot}2H_2O$ carried out in air generates α-Fe_2O_3 at 420°C. The process could be carried out in two stages – production of Fe_3O_4 and its oxidation at γ-Fe_2O_3. The transformation γ-Fe_2O_3–α-Fe_2O_3 has also been evidenced. The coprecipitation of Fe as an oxalate together with Bi, Sr, Ca, Cu does not modify the oxalates mixture coprecipitation conditions but some restrictions are required concerning the avoiding of the oxidation of Fe^{2+} at Fe^{3+} previously to the precipitation as an oxalate. The substitution of Cu by Fe in the material obtained by oxalate coprecipitation does not modify the precursor mixture decomposition mechanism, but determines changes in the mechanism formation of high-T_c superconducting phase.

References

1 Y. Metlin and Y. D. Tetryakov, J. Mater. Chem., 4 (1994) 1659.
2 M. Kakihana, J. Sol-Gel Sci. Technol., 6 (1996) 7.
3 H. Medelius and D. J. Rowcliffe, Mat. Sci. Eng., A109 (1989) 289.
4 G. Marbach, S. Stotz, M. Klee and J. W. C. de Vries, Phys. C, 161 (1989) 111.
5 C. Y. Shei, R. S. Liu, C. T. Chang and P. T. Wu, Mat. Lett., 9 (1990) 105.
6 N. D. Spencer, Chem. Mat., 2 (1990) 708.
7 M. Mansori, P. Satre, C. Breandon, M. Roubin and A. Sebaouin, Ann. Chim. Fr., 18 (1993) 537.
8 Y. Zhang, M. Muhammed, L. Wang, J. Nogues and K. V. Rao, Mat. Chem. Phys., 30 (1992) 153.
9 Y. Zhang, Z. Fang, M. Muhammed, K. V. Rao, V. Skumryev, H. Medelius and J. L. Costa, Phys. C, 157 (1989) 108.
10 C. Chiang, C. Y. Shei, Y. T. Huang, W. H. Lee and P. T. Wu, Phys. C, 17 (1990) 383.
11 L. Marta, M. Zaharescu, L. Ciontea and T. Petrisor, Appl. Supercond., 1 (1993) 677.
12 M. Chuanbin, D. Zehua and Z. Lian, Sci. in China, E39 (1996) 181.
13 M. Popa, A. Totovana, L. Popescu, N. Dragan and M. Zaharescu, J. Eur. Ceram. Soc., 18 (1998) 1265.
14 V. P. Danilov, O. N. Krasnobaeva, I. B. Kudinov, T. A. Nosova, V. M. Novotortsev and A. V. Filatov, Inorganic Mat., 30 (1994) 507.
15 L. Marta, O. Horovitz and M. Zaharescu, Key Eng. Mat. Vols 132–136, Trans. Tech. Publications, Switzerland 1997, p. 1239.
16 G. C. Nicholson, J. Inorg. Nucl. Chem., 29 (1967) 1599.
17 U. Kozo, J. Chem. Soc. Jap., 6 (1975) 1968.
18 D. Broadbent, D. Dollimore and J. Dollimore, J. Chem. Soc., 3 (1967) 451.
19 V. Rao, A. L. Shashimohan and A. B. Biswas, J. Mat. Sci., 9 (1974) 430.
20 A. Zuda, Thermochim. Acta, 8 (1974) 217.
21 B. Boyanov, D. Khazdhiev and V. Vasilev, Thermochim. Acta, 93 (1985) 89.
22 C. K. Hsu, J. S. Lee and C. W. Huang, J. Therm. Anal. Cal., 51 (1998) 295.
23 M. Popa, M. Zaharescu, L. Marta, L. Diamandescu and A. Totovana, Key Eng. Mat. Vols 132–136, Trans Tech Publications, Switzerland 1997, p. 1253.

24 M. Popa and M. Zaharescu, Rev. Roum Chim., 45 (2000) (in press).

25 M. Zaharescu, L. Marta, M. Popa and D. Crisan, Proc. of the 8th CIMTEC World Ceramics Congress and Forum on New Materials, ed. P. Vincenzini, Techna, Faenza, 1995, p. 409.

26 B. Boyanov, D. Khadzhiev and V. Vasilev, Scientific Works of Plovdiv University ‘P. Hilendarsky’, Himija.

27 M. Zaharescu, A. Braileanu, R. Manaila, V. Fruth and G. G. Tanase, Mat. Res. Bull., 27 (1992) 491.

28 M. Zaharescu, A. Braileanu and D. Crisan, J. Thermal Anal., 40 (1993) 321.

29 E. G. Derouane, Z. Gabelice, R. Hubin and M. J. Hubin-Frankin, Thermochim. Acta, 11 (1975) 287.

30 B. V. Strijkov, A. M. Lapitskii and L. G. Vlasov, Zh. Neorg. Khim., 7 (1962) 2352.

31 A. H. Verdonk, Thermal Analysis Vol. 2, Proc 3rd ICTA, Davos 1971, p. 651.

32 J. T. Yates and C. W. Garland, J. Phys. Chem., 65 (1961) 617.

33 L. Marta, M. Zaharescu and I. Haiduc, J. Thermal Anal., 41 (1994) 915.

34 V. P. Kormienko, Ukr. Chim. Zh., 23 (1957) 159.

35 P. Peshev, G. Gyurov, Y. Khristova, K. Petrov, D. Kovachvo, Y. Dimitriev, N. Nencheva and E. Evlakhor, Mater. Res. Bull., 23 (1988) 1765.

36 C. Duval, Inorganic Thermogravimetric Analysis, Elsevier Publishing, London 1963, p. 330.